Methods 59 (2013) 59–70

Contents lists available at SciVerse ScienceDirect

Methods

journal homepage: www.elsevier.com/locate/ymeth

Distinct gene expression signatures in human embryonic stem cells differentiated towards definitive endoderm at single-cell level

Karin Norrman [a,b,*], Anna Strömbeck [b], Henrik Semb [a,c], Anders Ståhlberg [d,e,*]

[a] Stem Cell and Pancreas Developmental Biology, Stem Cell Center, Department of Laboratory Medicine, Lund University, BMC B10, Klinikgatan 26, SE-22184 Lund, Sweden
[b] Cellartis AB, Arwid Wallgrens Backe 20, SE-41346 Gothenburg, Sweden
[c] The Danish Stem Cell Center, University of Copenhagen, Blegdamsvej 3B, Building 6, 4th Floor, DK-2200 Copenhagen N, Denmark
[d] Sahlgrenska Cancer Center, Department of Pathology, Sahlgrenska Academy at University of Gothenburg, P.O. Box 425, SE-40530 Gothenburg, Sweden
[e] TATAA Biocenter, Odinsgatan 28, SE-41103 Gothenburg, Sweden

ARTICLE INFO

Article history:
Available online 5 April 2012

Communicated by Michael W. Pfaffl

Keywords:
Human embryonic stem cells
Definitive endoderm
Gene expression profiling
RT-qPCR
Single-cell analysis
Single-cell biology

ABSTRACT

Characterization of directed differentiation of pluripotent stem cells towards therapeutically relevant cell types, including pancreatic beta-cells and hepatocytes, depends on molecular markers and assays that resolve the signature of individual cells. Pancreas and liver both have a common origin of anterior definitive endoderm (DE). Here, we differentiated human embryonic stem cells towards DE using three different activin A based treatments. Differentiation efficiencies were evaluated by gene expression profiling over time at cell population level. A panel of key markers was used to study DE formation. Final DE differentiation was also analyzed with immunocytochemistry and single-cell gene expression profiling. We found that cells treated with activin A in combination with sodium butyrate and B27 serum-free supplement medium generated the most mature DE cells. Cell population studies were useful to monitor the temporal expression of genes involved in primitive streak formation and endoderm formation, while single-cell analysis allowed us to study cell culture heterogeneity and fingerprint individual cells. In addition, single-cell analysis revealed distinct gene expression patterns for the three activin A based protocols applied. Our data provide novel insights in DE gene expression at the cellular level of in vitro differentiated human embryonic stem cells, and illustrate the power of using single-cell gene expression profiling to study differentiation heterogeneity and to characterize cell types and subpopulations.

1. Introduction

In the efforts of developing new sources of insulin producing cells for treatments of Type I diabetes, human embryonic stem cells (hESCs) hold a great promise as an unlimited source of insulin supply. Protocols for efficient generation of definitive endoderm (DE) and its subsequent differentiation to pancreatic progenitors and pancreatic β-cells (beta-cells) have been extensively reported [1–12]. Although, the cells generated with these protocols do not express the same combination of markers as their in vivo counterparts, glucose responsive beta-like cells can be generated when maturated in vivo [8]. This data indicate that hESCs have the potential to develop into functional insulin producing cells, but the instructive signals for in vitro maturation of pancreatic progenitors are missing. To overcome this challenge, it is generally believed that the most straightforward strategy of differentiating pluripotent stem cells towards beta-cells is to mimic the signaling pathways of pancreas development, during normal mammalian embryonic development, and to translate this knowledge to human in vitro systems.

The progressive developmental steps behind beta-cell differentiation are first initiated with formation of DE. In vertebrates, this process starts during gastrulation with the appearance of the primitive streak (PS) (reviewed in [13,14]). Pluripotent epiblast cells undergo epithelial to mesenchymal transitions and migrate through the PS and become either mesoderm or endoderm. The cells that first exit PS form the most anterior part of the embryo, while cells exiting later form the posterior part of the embryo. After migration through the PS, DE invades and replaces the extraembryonic endoderm layers of visceral endoderm (VE) that forms the supportive tissues of the embryo. During vertebrate gastrulation the Nodal signaling pathway regulates endoderm and mesoderm formation [15,16]. In the pregastrula embryo, high levels of Nodal induce endoderm and anterior mesendoderm, whereas low levels of Nodal

* Corresponding authors. Addresses: Cellartis AB, Arwid Wallgrens Backe 20, SE-41346 Gothenburg, Sweden, fax: +46 31 7580910 (K. Norrman); Sahlgrenska Cancer Center, Department of Pathology, Sahlgrenska Academy at University of Gothenburg, P.O. Box 425, SE-40530 Gothenburg, Sweden, fax: +46 31 828733 (A. Ståhlberg).
E-mail addresses: Karin.Norrman@cellartis.com (K. Norrman), anders.stahlberg@neuro.gu.se (A. Ståhlberg).

1046-2023/$ - see front matter © 2012 Elsevier Inc. All rights reserved.
http://dx.doi.org/10.1016/j.ymeth.2012.03.030

promote transcription of mesoderm and posterior endoderm. A key regulatory gene for PS formation is Brachyuru (*T*) that is induced by signals from extraembryonic endoderm [17,18]. Another transcription factor, Mix homeobox-like 1 (*Mixl1*), is expressed during gastrulation, when the early endoderm migrates out from the PS and plays an important role in cell commitment towards the endodermal linage and suppresses mesodermal differentiation [19]. *Mixl1* is also required for cell movement that during gastrulation is associated with anterior expansion of DE and gut tube morphogenesis [19,20]. Cerberus 1 (*Cer1*), SRY (sex determining region Y)-box 17 (*Sox17*) and forkhead box A2 (*Foxa2*) are expressed in DE and are in many aspects key regulatory genes for endoderm development and specification of foregut endoderm, the part of the endoderm that later on gives rise to organs, such as pancreas and liver [21,22]. Absence of *Sox17* in mice results in depletion of DE in the foregut endoderm [23]. In the pre/early-streak embryo, *Sox17* is expressed in the entire extraembryonic/VE endoderm. At mid-streak stage *Sox17* is expressed in endoderm at the anterior end of the PS, but not in VE. At the time of DE movement to the anterior gastrula, *Sox17* expression expands more anterior and is therefore specifically expressed in DE of the gastrula in contrast to other endoderm markers such as *Cer1*, *Foxa2* and hematopoietically-expressed homeobox protein (*Hhex*) that are also expressed in anterior VE [21,22]. The C-X-C chemochine receptor type 4 (*Cxcr4*) is expressed in DE and in mesoderm but not in VE [24–26]. After gastrulation, the endoderm is regionalized along the anterior–posterior axis into foregut, midgut and hindgut, where foregut later on is specified into thyroid, lung, hepatic and pancreatic endoderm. *Hhex* is one of the earliest markers that regulates anterior–posterior identity and is expressed in the first anterior DE cells, emerging from the PS [27], and plays an essential role in maintaining anterior identity [28,29]. Moreover, at late gastrulation, LIM homeobox 1 (*Lhx1*), orthodenticle homeobox 2 (*Otx2*), *Cer1* and *Foxa2* have been shown to be required for establishment of the anterior–posterior axis body plan [30–32]. *Sox17*, *FoxA2*, *Hhex* and *Cer1* are all expressed both in DE and VE, while SRY (sex determining region Y)-box 7 (*Sox7*) is exclusively expressed in mouse VE [23]. Markers that are expressed during regionalization of the gut endoderm include alpha fetoprotein (*Afp*) [33], caudal type homeobox 2 (*Cdx2*) [34] and HNF1 homeobox B (*Hnf1b*) [35]. To summarize, genetic studies in vertebrates have shown that there is no exclusive markers that can be used to define anterior DE, which is the origin of both beta-cells and hepatocytes. Instead, cell characterization relies on using a combination of markers that collectively identifies anterior DE and excludes a VE phenotype.

In the attempts of translating developmental biology into strategies for in vitro differentiation of pluripotent stem cells, research tools that define the molecular events within heterogeneous cell populations are needed. Individual cells in a seemingly homogenous cultures or tissues are in many aspects unique in their expression of transcripts and proteins [36]. This implies that cell population data cannot be used to accurately describe individual cells. Immunocytochemistry provides an opportunity to specifically target cells expressing anterior DE markers at the protein level. However, there are few or no published data using these antibodies for immunolocalization in hESCs. Furthermore, only a few proteins may be analyzed simultaneously using immunocytochemistry. This highlights the need for novel assays and tools that, at cellular level, monitor differentiation of hESCs towards DE. The use of single-cell gene expression analysis to understand stem cell heterogeneity and the dynamic transition between cell fates has been recognized for a long time, but lack of analytical techniques sensitive enough to measure few transcripts has limited such experiments. However, recent advances allow robust and reproducible single-cell gene expression measurements to be performed [37–39].

Here, we differentiated hESCs towards DE using three different activin A based protocols. The dynamics of DE markers were analyzed over time using gene expression profiling at cell population level. The temporal analysis of DE associated markers identified an optimal endpoint stage of differentiation that was further characterized by single-cell gene expression profiling. Immunocytochemistry was used to confirm expression of DE markers at protein level. Analysis of multiple markers associated with differentiation at the single-cell level allowed us to determine characteristic transcript signatures for cells generated by the three different activin A treatments. Our data illustrate the value of analyzing multiple markers at the cellular level and how single-cell analysis can be implemented as a research tool to understand hESC differentiation.

2. Material and methods

2.1. Cell cultures and differentiation of human embryonic stem cells

The hESC line SA121 [40] was maintained as undifferentiated cells in DEF™-CS (Cellartis AB), according to Swedish ethics guidelines. For differentiation, hESCs were passaged into differentiation media, containing RPMI1640 (Gibco, Invitrogen) supplemented with 0.1% Penicillin/Streptomycin (Gibco) and activin A 100 ng/ml (Peprotech), up to 7 days according to Fig. 1. For AAFBS, differentiation medium supplemented with 0.2% fetal bovine serum (Sigma–Aldrich) was used day 0–2 and 1% fetal bovine serum was used day 3–7. For the AAB27 and AANaB protocols, differentiation medium was supplemented with 2% B27 serum-free supplement medium (Gibco) all days. In AANaB, 1 mM sodium butyrate (NaB, Sigma–Aldrich) was added day 0–1 and 0.5 mM NaB day 2–7 [12]. Full medium change was performed every day. Bright field images of cells were taken on an inverted microscope (Eclipse TE2000-U, Nikon).

2.2. Immunocytochemistry

Cells were washed once in phosphate buffered saline and fixed in 4% paraformaldehyde for 15 min, washed three times in PBS, permeabilized in 0.5% TritonX-100 for 15 min (all Sigma–Aldrich). Primary antibodies: goat anti-SOX17 (1:500) (R&D Systems), mouse anti-POU5F1 3/4 (1:200, Santa Cruz), mouse anti-AFP (1:500, Sigma–Aldrich), goat anti-FOXA2 (1:500, Santa Cruz Bio-

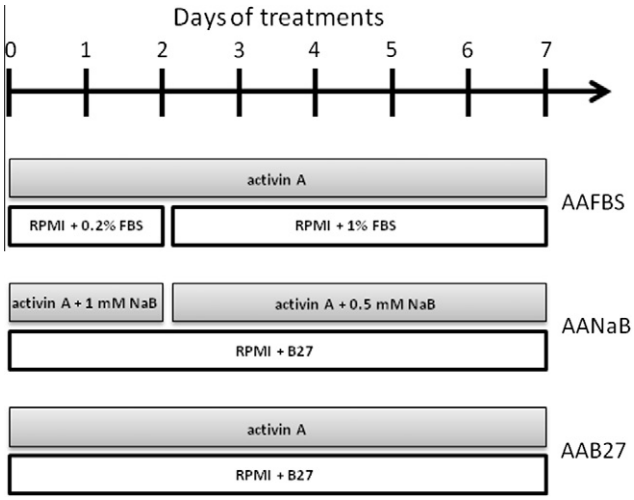

Fig. 1. Definitive endoderm differentiation. Human embryonic stem cells were treated with activin A using three different protocols: AAFBS, AAB27 and AANaB to induce differentiation towards definitive endoderm. Detailed differentiation protocols are described in Section 2.

technology), mouse anti-CDX2 (1:200, BioGenex 1/200) and goat anti-Sox7 (1:200) (R&D Systems) were incubated in phosphate buffered saline at 4 °C over night. As secondary antibodies, Alexa Fluor 594 conjugated donkey-anti-rabbit IgG, Alexa Fluor 488 donkey-anti-goat IgG, Alexa Fluor 488 donkey-anti-rabbit IgG and Alexa Fluor 488-α-mouse IgG (all Molecular Probes) were added in a 1:500 dilution in phosphate buffered saline for 1 h at room temperature. Cell nuclei were stained with DAPI (Sigma–Aldrich). Immunostained cells were visualized with Nikon Eclipse TE2000-U Fluorescence microscope and Nikon Act-1C for DXM1 200C software.

2.3. Total RNA extraction and reverse transcription

Cells were harvested in RNA Cellprotect (Qiagen) every day for all differentiation protocols. Total RNA was extracted using the RNeasy mini-Kit (Qiagen), following the standard protocol for animal cells. Removal of residual genomic DNA from all samples was done with DNase I treatment (Qiagen), according to the manufacturer's protocol. Reverse transcription was performed using 200 ng total RNA in a final volume of 20 µl, using HighCapacity cDNA Reverse Transcription Kit (Applied Biosystems) using Rotorgene 3000 (Qiagen), according to manufacturer's instructions. Each cDNA sample was diluted with water to 200 µl.

2.4. Gene expression profiling

LightCycler 480 (Roche Diagnostics) and ABI PRISM 7900 HT sequence detection system (Applied Biosystems) were used for gene expression profiling following the minimum information for publication of quantitative real-time PCR [41]. Both TaqMan based probe and SYBR Green I assays were used. Detailed assay information is shown in Table S1. For SYBR Green I based assays, iQ SYBR Green Supermix (Bio-Rad) and 400 nM of each primer (Sigma–Aldrich) was used and the applied temperature profile was 95 °C for 3 min followed by 50 cycles of amplification (95 °C for 20 s, 60 °C for 20 s and 72 °C for 20 s). For TaqMan probe based assays, TaqMan Gene Expression Master Mix with UNGase and 1× TaqMan primer/probe mix for respective gene was used (both Applied Biosystems). The temperature profile for TaqMan assays was 50 °C for 2 min and 95 °C for 10 min followed by 40 cycles of amplification (95 °C for 15 s and 60 °C for 1 min). Assay performance was evaluated with standard curve (Figs. S1 and S2). All SYBR Green I generated data were confirmed with melting curve analysis. No assay amplified genomic DNA, tested by reverse transcription negative samples. Potential references genes were evaluated using NormFinder and GeNorm algorithms. Data were normalized against the geometric mean expression of *ACTB*, *RPL7*, *RPS10* and *YWHAZ*. The comparative Cycle of quantification (Cq) method for relative quantification (ΔΔCq-method) was used and performed as described [42]. Gene expression levels were plotted as mean ± SD of three independent biological experiments.

2.5. Single-cell gene expression profiling

Single-cell sorting for gene expression profiling has been described elsewhere [38,43,44]. Briefly, hESCs were enzymatically dissociated into single-cell suspensions and kept in differentiation medium on ice until cell sorting. Single-cells were sorted with BD FACSAria (BD Biosciences) into 96-well plates containing 5 µl CelluLyser (TATAA Biocenter) per well. Samples were frozen at 80 °C until subsequent analysis. Transcriptor (Roche Diagnostics) was used for reverse transcription. Lysed single-cells in 13 µl water containing 2.5 µM anchored-oligo(dT18) primer and 3.0 µM random hexamers (both Roche Diagnostics; final concentrations) were incubated at 65 °C for 5 min; 1× reaction buffer with 8 mM $MgCl_2$, 1 mM deoxynucleotide mix, 20 U Protector RNase inhibitor and 10 U Transcriptor (all Roche Diagnostics; final concentrations) were added to a final volume of 20 µl. Reverse transcription was performed at 25 °C for 5 min, 50 °C for 60 min, 55 °C for 15 min and terminated by heating to 85 °C for 5 min. Pre-amplification with 10 µl cDNA and 25 nM of each primer was performed in 100 µl, using iQ SYBR Green Supermix (Bio-Rad). Primers for the following genes were included: *CDX2, CER1, CXCR4, FOXA2, HHEX, HNF1B, LHX1, MIXL1, NANOG, POU5F1* and *SOX17* (Sigma–Aldrich). Primer sequences are provided in Table S1. The temperature profile was 95 °C for 3 min followed by 15 cycles of amplification (95 °C for 20 s, 55 °C for 20 s and 72 °C for 3 min). Samples were immediately frozen on dry ice after finishing the last elongation step. All samples were diluted 1:10 with water before qPCR. LightCycler 480 (Roche Diagnostics) was used for all qPCR measurements. To each 10 µl reaction, containing iQ SYBR Green Supermix (Bio-Rad) and 400 nM of each primer (Table S1), we added 3 µl of diluted pre-amplified cDNA. The temperature profile was 95 °C for 3 min followed by 50 cycles of amplification (95 °C for 20 s, 60 °C for 20 s and 72 °C for 20 s). The formation of expected PCR products was confirmed by melting curve analysis and all assays were verified by agarose gel electrophoresis. Performance of pre-amplification and qPCR assays used for single-cell measurements are shown in Fig. S2.

2.6. Single-cell analysis

Distributions of transcripts are lognormally distributed in single-cells [38,39,45]. The Cq-values represent the negative logarithmic transcript number in qPCR measurements. Consequently, all single-cell data analyses were performed with Cq-values. For hierarchical clustering, principal component analysis (PCA) and Kohonen self-organizing maps complete data matrices were needed. For these analyses, cells without expression of a specific marker where given a Cq-value of the maximum Cq-value quantified for that particular gene plus two. A few cells had contribution of unspecific PCR products. These cells received a Cq-value of the maximum Cq-value quantified for that particular gene plus one. All data analyses were robust and were not found to depend on missing data strategy as long as missing data were considered to represent cells with transcript levels below level of detection for respective assay. All Cq-values were mean-centered for respective gene in Fig. 6 and Table 1. Consequently, a negative mean-centered Cq-value corresponds to a cell with expression above the overall mean for that particular gene. Spearman correlation was performed in SPSS (16.0 or later, SPSS Inc.) software. Hierarchical clustering, PCA and Kohonen self-organizing maps were performed in GenEx software (MultiD). Expression of each gene was autoscaled for hierarchical clustering analysis, using Ward's algorithm and Euclidean distance measure. Autoscaled gene expression values were also used in PCA to give all genes equal weight in the clustering algorithms. The data were analyzed as described [38,42].

3. Results

3.1. Dynamics of global gene expression during differentiation towards DE

To induce differentiation towards DE, hESCs (cell line SA121) were treated with activin A, a member of the TGF-b superfamily that mimics Nodal signaling [46,47]. Three different activin A treatments were used as illustrated in Fig. 1. Briefly, in the AAFBS protocol, hESCs were differentiated with activin A and low concentration of fetal bovine serum [3]. The serum was replaced with B27 serum-free supplement medium in the AAB27 protocol

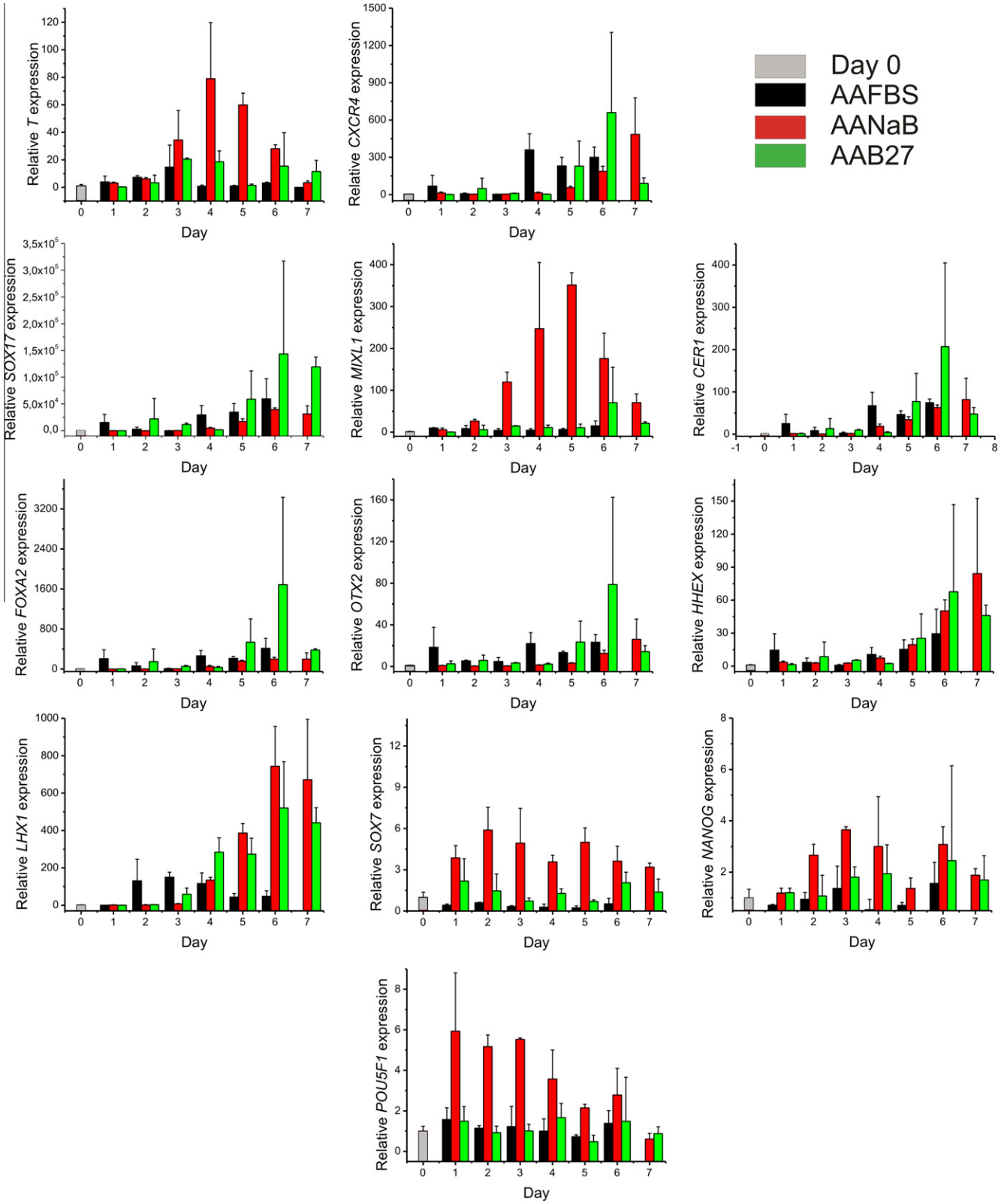

Fig. 2. Temporal analysis of gene expression at cell population level during AAFBS, AANaB and AAB27 treatments. Optimal endpoint of DE differentiation for AAFBS treated cells was day 5 and 7 for AAB27 and AANaB treated cells. Data for AAFBS treated cells at day 7 are missing, due to poor cell survival. Data are shown as mean ± SD of three independent experiments. The expression value was arbitrarily set to a value of 1 for all genes at day 0. Note the difference in scale for respective gene.

and with B27 serum-free supplement medium and sodium butyrate (NaB) in the AANaB protocol [12]. Expression of genes involved in PS formation and differentiation towards anterior DE were monitored under 7 days using reverse transcription quantitative real-time PCR (Fig. 2). The expression profile of PS and DE markers in AAB27 and AANaB treated cells showed similar

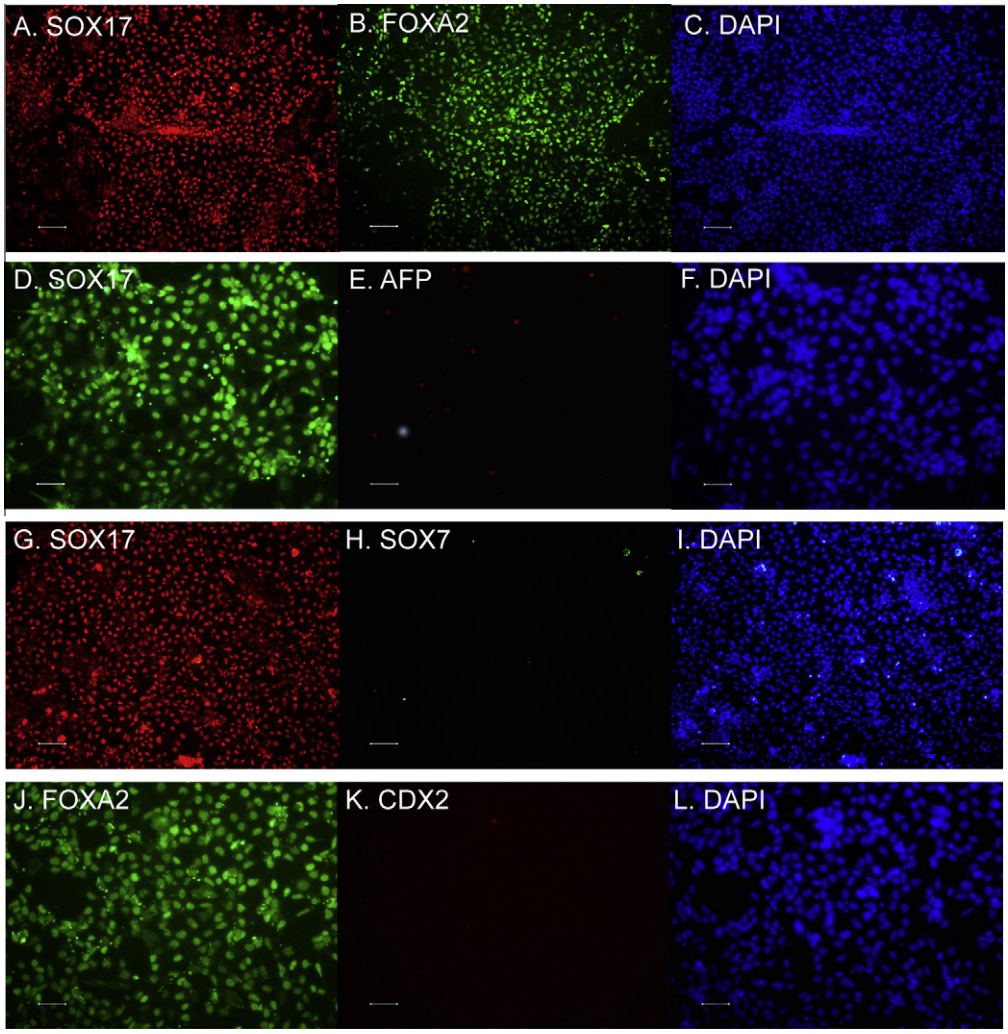

Fig. 3. Immunocytochemistry analysis at endpoint stage for AANaB treated cells. The majority of SOX17$^+$ cells co-expressed FOXA2 (A–C). AFP (D–F) and SOX7 (G–I) were not detected in SOX17 expressing cells. CDX2 was not detected in FOXA2+ cells (J–L). Cells were counterstained with DAPI for nuclear localization. Scale bar in (A–C) and (G–I) represent 100 μm and 50 μm in (D–F) and (J–L).

dynamics as during vertebrate endoderm differentiation [14], while the gene expression profile of AAFBS treated cells did not follow the temporal expression pattern found in mouse development. The gene regulation differed in magnitude between the treatments, where most DE genes were induced to lower levels in AAFBS treated cells than in AANaB and AAB27 treated cells, indicating a less efficient method for DE differentiation. The PS gene, *T*, which is involved in segregating mesoderm and endoderm, was transiently expressed day 3–7 in both AAB27 and AANaB treatments (Fig. 2). In AANaB treated cells, *T* was clearly downregulated day 7, which indicate differentiation towards endodermal rather than to mesodermal cell types. The expression of *MIXL1* followed the expression pattern of *T*, during AANaB differentiation. In AAB27 treated cells, *MIXL1* was upregulated first at day 6, while AANaB treated cells upregulated *MIXL1* already day 3. The transient gene expression pattern of PS markers was followed by upregulation of a panel of DE genes (*CER1*, *CXCR4*, *HHEX*, *FOXA2*, *OTX2* and *SOX17*). In AAB27 and AANaB treated cells, the endodermal genes *SOX17* and *FOXA2* were induced at day 5–7 and both were expressed at slightly higher levels in the AAB27 treated cells (Fig. 2). In addition, induction of *CXCR4* was also induced at day 5–7. According to the expression pattern found in mouse, Cxcr4 is expressed in early endoderm and mesoderm but not in anterior VE. Thus, upregulation of *SOX17*, *FOXA2* and *CXCR4* indicated differentiation towards DE rather than VE, during AAB27 and AANaB treatments. Furthermore, the VE marker *SOX7* did not follow the induction pattern observed for the DE genes. Notably, cells that were differentiated in the absence of activin A showed upregulation of *SOX7* expression, while the expression of DE genes were downregulated compared to activin A differentiated cells (Fig. S3). These data support the hypothesis that activin A promotes differentiation towards DE but not VE. Moreover, the markers involved in anteriorization of DE: *CER1*, *HHEX*, *LHX1* and *OTX2*, were upregulated at day 5–7, the same time as the other DE genes were upregulated and indicated specification of anterior DE during AAB27 and AANaB treatments (Fig. 2). The *LHX1* expression peaked at day 6–7 for AAB27 and AANaB treatments, while AAFBS treated cells showed an overall low *LHX1* expression throughout all days. *CDX2* was absent in most analyzed samples, regardless days of differentiation (data not shown).

In summary, anterior DE markers (*CER1, HHEX, LHX1* and *OTX2*) were induced at the same time as universal DE genes (*SOX17, FOXA2*) for both AAB27 and AANaB treatments, while the PS markers *T* was only downregulated for AANaB treated cells. This gene expression pattern is similar to PS/mesendoderm formation and the following development of anterior DE, during mouse development [14]. At day 7, all DE genes were induced, while pluripotency

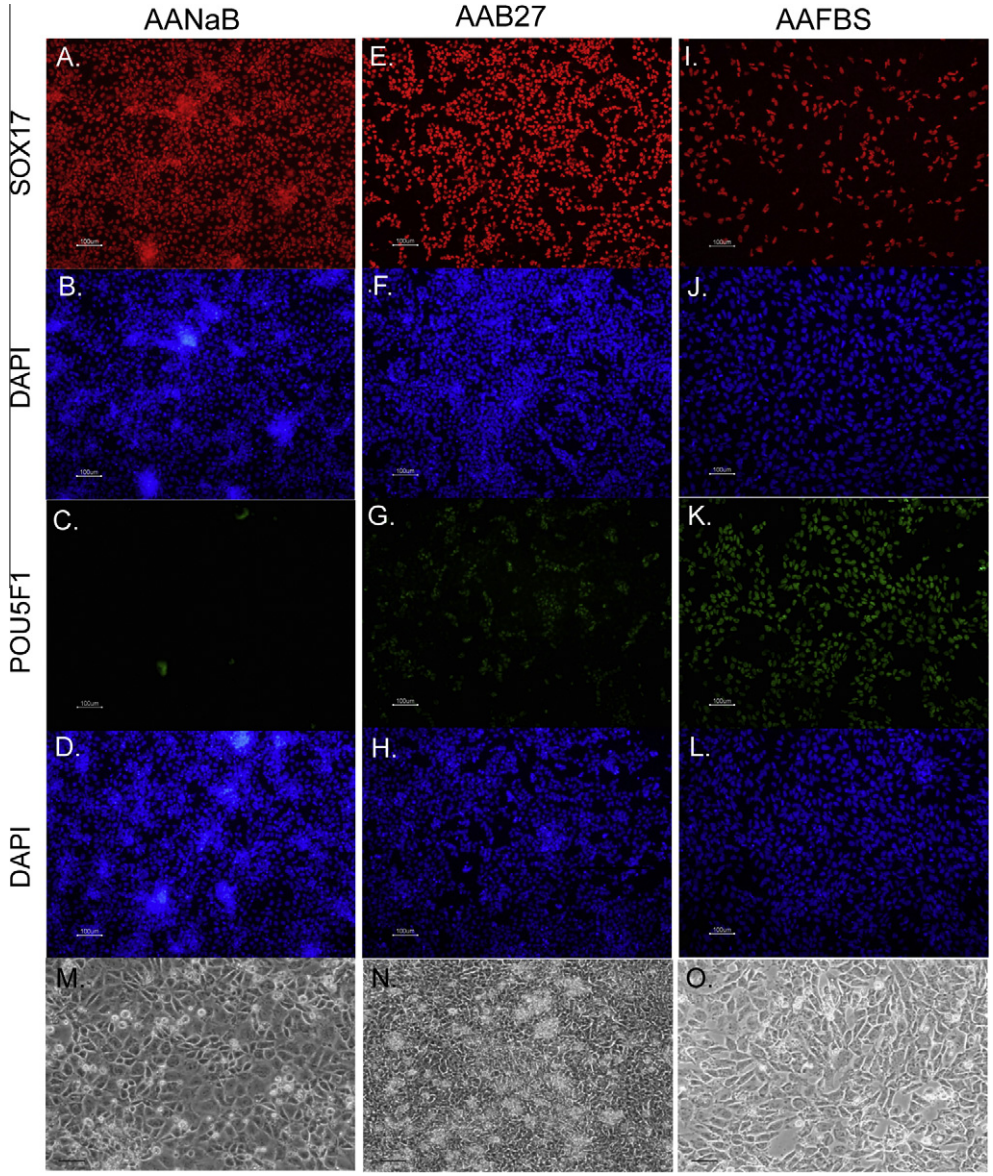

Fig. 4. Immunocytochemistry analysis at endpoint stage of DE differentiation. SOX17 and POU5F1 expression in AANaB (A–D), AAB27 (E–H) and AAFBS (I–L) treated cells at endpoint stage. Endpoint stage for AANaB and AAB27 treated cells were day 7 and 5 for AAFBS treated cells. Cells were counterstained with DAPI for nuclear localization. Bright field images show cellular morphologies at endpoint stage of differentiation in each treatment (M–O). Scale bars in panels (A–L) represent 100 μm and in panels (M–O) represent 50 μm.

markers POU domain class 5 transcription factor 1 (*POU5F1*, also known as *OCT4*) and Nanog homeobox (*NANOG*) remained unregulated. Therefore, we chose day 7 to study the differentiation capacity of the AAB27 and the AANaB treated cells in detail with immunocytochemistry and single-cell analysis. Day 5 was chosen for AAFBS treated cells, according to the same criteria. In addition, these cells started to die after day 5.

3.2. Immunocytochemistry showed efficient differentiation towards DE but not to extraembryonic and gut endoderm

To qualitatively analyze differentiation, immunostainings were performed at endpoints stage of each treatment (Fig. 3). The majority of the AANaB treated cells co-expressed SOX17 and FOXA2. AFP and CDX2 that are expressed in the gut endoderm tube in mouse were not detected at day 7 in AANaB treated cells, indicating that these cells have not developed into gut endoderm. In addition, the VE marker SOX7 was not detected in AANaB cultures, supporting the observation that *SOX7* gene expression were not efficiently upregulated during activin A treatment. Similar results were observed in AAB27 treated cells (Fig. S4). Most AANaB and AAB27 treated cells were $SOX17^{+}$ and $POU5F1^{-}$, but a somewhat higher portion of $POU5F1^{+}$ cells were observed in the AAB27 treated cultures (Fig. 4). AAFBS treated cells showed fewer $SOX17^{+}$ cells and less efficient downregulation of POU5F1 compared to AAB27 and AANaB treated cells.

3.3. Distinct morphology of DE differentiated cells

During the first 24 h of AANaB treatment a dramatic cell death was observed, where surviving cells started to proliferate from day 4 and reached confluence at day 7. AANaB treated cells showed marked changes in cellular morphology over time and were homogenous at day 7, where individual cells exhibited uniform

morphology illustrated by bright field images in Fig. 4M. This morphology and homogeneity was not observed to the same extent in AAB27 treated cells (Fig. 4N). The AAFBS treated cells were grown to confluence around day 3–5 as illustrated in Fig. 4O. Thereafter, the number of cells gradually declined.

3.4. Single-cell gene expression analysis revealed distinct SOX17 positive cell populations

Eighty-two single-cells from respective activin A treatment were collected by flow cytometry, lysed, reverse transcribed, pre-amplified and analyzed with quantitative real-time PCR. Performance of the pre-amplification step is shown in Fig. S2. Gene expression of *CDX2, CER1, CXCR4, FOXA2, HHEX, HNF1B, LHX1, MIXL1, NANOG*, *POU5F1* and *SOX17* were analyzed. All single-cells were negative for *CDX2* expression, which is in agreement with the immunostainings (Fig. 3). Basic statistical parameters for all single-cell data are described in Table 1.

Initially, we performed binary data analysis at the single-cell level to identify co-expression of PS and DE genes with *SOX17* (Table 2). Here, we used *SOX17* as key marker for DE differentiation, since *SOX17* is only expressed in endoderm, and exclusively expressed in DE from mid-streak stage embryo [23]. Sixty percent of the AAB27 treated cells expressed *SOX17* and 71% of these cells expressed the mesendodermal marker *CXCR4*. Co-expression of *SOX17* and *CXCR4* excluded VE being formed. The corresponding number for AANaB treated cells was 63%. During AAB27 differentiation all *SOX17*$^+$ cells co-expressed *CER1*. The percentages for *FOXA2*, *HHEX*, *MIXL1* and *LHX1* were 82%, 69%, 86% and 73%, respectively (Table 2). The pluripotency markers *POU5F1* and *NANOG* were co-expressed in 59% of the *SOX17*$^+$ cells (*SOX17*$^+$*POU5F1*$^+$*NANOG*$^+$ cells).

During AANaB differentiation 63% of the cells expressed *SOX17*. Ninety-six percent of the SOX17$^+$ cells co-expressed *CER1* and *FOXA2*, respectively, whereas 57% expressed *HHEX* (Table 2). Moreover, *CXCR4* was detected in 86% of the *SOX17*$^+$ cells and pluripotency markers *POU5F1* and *NANOG* were co-expressed in 33% of the *SOX17*$^+$ cells (*SOX17*$^+$*POU5F1*$^+$*NANOG*$^+$ cells). Interestingly, AANaB treatment generated 55% *SOX17*$^+$*MIXL1*$^+$ cells and 37% *SOX17*$^+$*LHX1*$^+$ cells, which were lower percentages compared to AAB27 treated cells (86% and 73%, respectively).

During AAFBS differentiation, the majority of the cells co-expressed *CER1, POU5F1* and *NANOG* (data not shown). *SOX17* expression was only detected in 5 of the 82 (6%) analyzed cells. Within the *SOX17*$^+$ population, *CER1*, *CXCR4, FOXA2* and *HHEX* were co-expressed in 2 of the 5 *SOX17*$^+$ cells. In all activin A treatments, *HNF1B* was expressed in less than 4 cells regardless differentiation protocol and was therefore not included in further correlation and classification analysis (Table 1). Of the *HNF1B* positive cells detected, all cells co-expressed *CER1*, *CXCR4*, *FOXA2*, *LHX1* and *SOX17* independent of differentiation method.

Conclusively, both AAB27 and AANaB treatments generated similar numbers of cells co-expressing DE markers: *CER1*, *CXCR4, FOXA2*, *HHEX* and *SOX17*. However, the *SOX17*$^+$ population generated during AAB27 differentiation co-expressed *LHX1* and *MIXL1* transcripts to higher extent compared to AANaB differentiation. In contrast, pluripotency genes were more rarely expressed in the *SOX17*$^+$ population generated, during AANaB differentiation.

3.5. Single-cell gene expression profiling revealed cellular heterogeneity

High variability in gene expression was observed both within and between the three different activin A treatments, indicating a non-synchronized differentiation (Fig. 5). Hierarchical clustering of all cells, regardless activin A treatment used, grouped DE genes (*CER1, CXCR4, FOXA2, HHEX*, *LHX1*, *MIXL1* and *SOX17*) together, where the expression profile of *SOX17* and *FOXA2* were most similar. The pluripotency markers *POU5F1* and *NANOG* grouped separately (Fig. 5).

The relative transcript levels for respective gene and treatment are presented in Fig. 6. Several genes showed 10,000-fold variation or higher in transcript levels both within and between differentiation protocols. The observed differences between activin A treatments at cell population level were to a large extent also observed when analyzing the positive population of a given gene at single-cell level. The relative gene expression levels of most DE genes were observed at similar or somewhat lower levels in AAFBS treated cells compared to AAB27 and AANaB treated cells at cell population level (Fig. 2). The number of cells expressing DE genes was significantly lower in AAFBS treated cells (Table 1), but the transcript levels of the positive cells were in the same range as for the other treatments (Fig. 6). These data suggest that the lower expression level observed at cell population level in AAFBS treated cells could be explained by fewer cells expressing a specific gene but at expression levels similar to the other treatments. The distributions of *MIXL1* and *LHX1* for AAFBS differentiation were in agreement with cell population analysis, whereas in AAB27 and AANaB treatments, the distribution of respective gene was more unclear compared to the global analysis. The relative distribution of *MIXL1* and *LHX1* transcripts showed a skewed expression towards higher levels in AAB27 treated cells compared to AANaB treated cells (Fig. 6). This was not as obvious when comparing *MIXL1* and *LHX1* expression at cell population level (Fig. 2). By comparing the gene expression profile at single cell level to the profile at cell population level, we conclude that global cell

Table 1
Statistical parameters describing gene expression in single cells using AAFBS, AAB27 and AANaB differentiation protocols.

Gene	AAFBS		AANaB		AAB27	
	n[a]	Mean[b]	n[a]	Mean[b]	n[a]	Mean[b]
CER1	46	−0.73	60	0.90	77	0.27
CXCR4	18	−0.17	48	1.09	35	−1.41
HNF1B	2	−0.21	3	0.14	3	0.00
POU5F1	51	−2.04	47	3.94	78	−0.71
HHEX	8	0.37	32	0.92	39	−0.76
MIXL1	21	0.67	32	2.10	61	−0.80
SOX17	5	−0.25	52	1.09	49	−1.13
FOXA2	8	0.15	61	0.00	50	−0.26
LHX1	4	0.40	22	0.96	38	−0.61
NANOG	44	−1.55	54	2.01	62	−0.17

[a] Number of cells expressing a given gene. $n_{tot} = 82$ for respective treatment.
[b] Mean gene expression of respective treatment. All numbers are expressed as cycle of quantification values ($\log_2$-scale) and values are mean-centered for respective gene. Negative values represent expression above the mean for that particular gene. For example, the mean expression of *CER1* in AAFBS treated cells was $1.92^{(0.90-(-0.73))} = 2.9$ times higher than in AANaB treated cells, using the assay specific PCR efficiency of *CER1* (Table S2).

Table 2
Binary analysis of the *SOX17* positive cell population.

Gene	AANaB[a] (%)	AAB27[a] (%)
CER1	96	100
CXCR4	86	71
POU5F1	47	61
HHEX	57	69
MIXL1	55	86
FOXA2	96	82
LHX1	37	73
NANOG	61	63

[a] Percent of cells expressing a given gene in the *SOX17* positive cell population for cells treated with AANaB and AAB27.

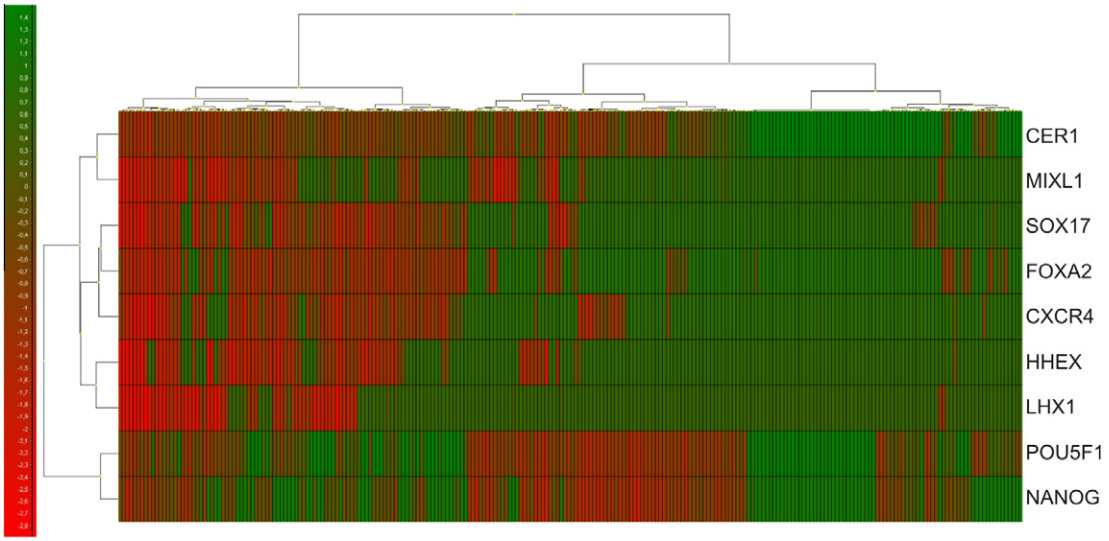

Fig. 5. Cell heterogeneity and gene clustering. Heat map of hierarchical clustering grouped differentiation genes (*CER1*, *CXCR4*, *FOXA2*, *HHEX*, *LHX1*, *MIXL1* and *SOX17*) together, where the expression profile of *SOX17* and *FOXA2* were the most similar, while *POU5F1* and *NANOG* grouped separately. Gene expression levels of all genes were autoscaled Cq-values. High expression is shown in red (negative values), while low expression is shown in green (positive values).

Table 3
Spearman correlation coefficients for AAFBS, AANaB and AAB27 treated cells.

	CER1	*CXCR4*	*POU5F1*	*HHEX*	*MIXL1*	*SOX17*	*FOXA2*	*LHX1*	*NANOG*
AAFBS									
CER1	1								
CXCR4	0.55	1							
POU5F1	0.30	−0.15	1						
HHEX	0.31	0.00	−0.21	1					
MIXL1	0.19	0.40	−0.64	–	1				
SOX17	–	–	−0.40	–	–	1			
FOXA2	0.77	**1.00**	−0.31	–	–	–	1		
LHX1	–	–	–	–	–	–	–	1	
NANOG	**0.55**	−0.24	**0.72**	−0.21	−0.57	–	0.10	–	1
AANaB									
CER1	1								
CXCR4	**0.66**	1							
POU5F1	−0.27	0.37	1						
HHEX	0.19	0.22	0.37	1					
MIXL1	0.12	−0.25	0.60	−0.18	1				
SOX17	**0.41**	0.36	0.03	0.12	0.38	1			
FOXA2	0.33	0.20	−0.09	0.26	0.13	0.22	1		
LHX1	−0.44	−0.06	−0.04	−0.49	0.09	031	−0.22	1	
NANOG	−0.33	0.16	**0.73**	0.20	0.49	0.14	0.22	−0.00	1
AAB27									
CER1	1								
CXCR4	**0.50**	1							
POU5F1	**−0.42**	0.08	1						
HHEX	**0.55**	0.39	0.14	1					
MIXL1	**0.59**	0.35	−0.01	**0.45**	1				
SOX17	**0.43**	0.14	0.14	**0.52**	0.32	1			
FOXA2	**0.62**	**0.57**	−0.17	**0.46**	**0.55**	**0.57**	1		
LHX1	**0.61**	−0.41	0.26	0.48	**0.46**	**0.46**	**0.60**	1	
NANOG	**−0.35**	0.15	**0.69**	0.10	−0.23	0.17	−0.20	0.23	1

Bold indicates ⩾99% significance; underline indicates ⩾95% significance. Correlation coefficients were not calculated for gene pairs with fewer than five data points.

population analysis could not in all cases provide sufficient resolution to detect differences between treatments.

3.6. Expression of anterior DE genes correlated at the cellular level during AAB27 treatment

Spearman correlation analysis was performed at the single-cell level to find common gene expression patterns within respective activin A treatment (Table 3). A correlation coefficient of 1 reflects perfect correlation, −1 reflects perfect anti-correlation and 0 is no correlation. Notably, the DE genes showed an overall positive correlation ($P \leqslant 0.05$) at the cellular level in AAB27 differentiated cells. In the AANaB cells, only four correlations between DE genes (*CER1*:*CXCR4*, *CER1*:*SOX17*, *CER1*:*FOXA2* and *CXCR4*:*SOX17*) were found ($P < 0.05$), compared to 17 positive correlations for the AAB27 treated cells ($P < 0.05$). In addition, *CER1* was negatively

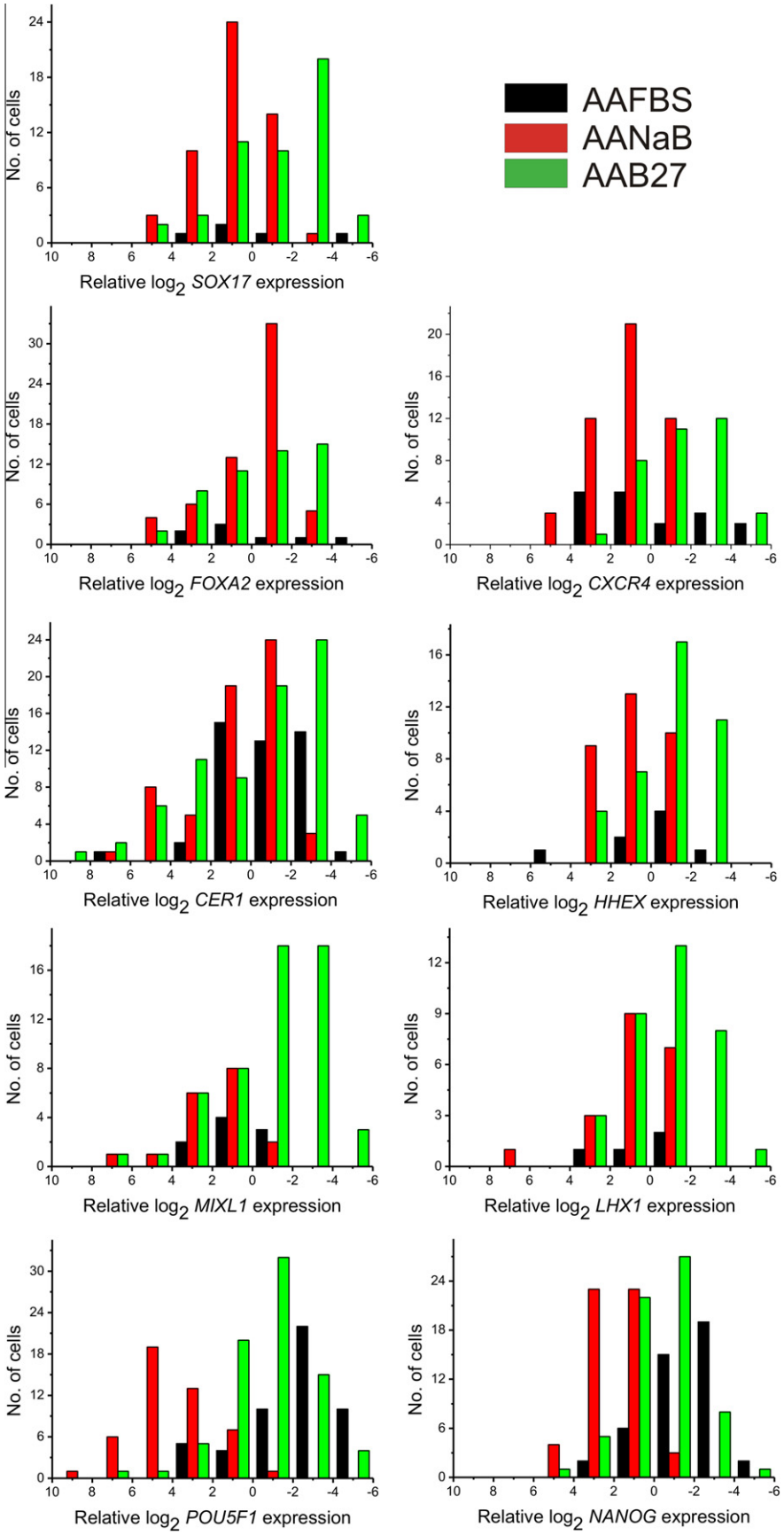

Fig. 6. Gene expression levels for AAFBS, AANaB and AAB27 treated cells at single-cell level. Distributions are shown as relative gene expression levels per cell plotted in $\log_2$-scale. Data are expressed as mean-centered cycle of quantification (Cq) values and are inversely proportional to transcript numbers.

correlated with the pluripotency markers *POU5F1* and *NANOG* for AAB27 treated cells. In AAFBS treated cells, two positive correlations were detected between the DE genes (*CER1*:*CXCR4* and *CXCR4*:*FOXA2*). In all activin A treatments, expression of pluripotency genes *POU5F1* and *NANOG* positively correlated to each other. Additionally, there was no or negative correlations between pluripotency genes and endodermal genes in AAB27 and AANaB treated cells. In summary, correlation data showed that the expression of DE genes were synchronized in AAB27 treated cells, while the expression of DE markers in AANaB and AAFBS cells were mainly non-synchronized.

3.7. Individual cells grouped into different subpopulations based on treatment protocol

To test if individual cells from the different treatment protocols could be classified into different subpopulations based on their gene expression profiles, we applied principal component analysis (PCA) (Fig. 7). PCA is an unsupervised learning algorithm. To give all genes equal importance in the classification analysis all data were autoscaled [42]. PCA revealed three different subpopulations of cells. Interestingly, the individual cells mainly grouped according to their treatment. Most AAFBS cells were grouped together and these cells were characterized by low anterior DE expression levels and high expression levels of pluripotency genes (Table 1 and Fig. 6 and Fig. S5). The subpopulation with AANaB treated cells showed intermediate expression of anterior DE genes and low expression of pluripotency genes, while cells treated with AAB27 were characterized with high levels of both anterior DE and pluripotency markers (Table 1 and Fig. 6 and Fig. S5). However, all activin A treatments were represented with at least a few cells in respective subpopulation defined by PCA, indicating that all three treatments could generate the same cell types, but with different efficiency. Single-cell grouping by PCA (Fig. 7) mainly overlapped with the hierarchical clustering shown in Fig. 5 (data not shown). We also applied Kohonen self organizing maps to screen for more subpopulations [38]. This screen identified two subpopulations, one subpopulation characterized by low expression of DE markers and high expression of pluripotency markers, while the cells in the other subpopulation were represented by low expression of pluripotency markers and high expression of DE markers. Many cells were also found to be in transition between an undifferentiated and differentiated cell state (data not shown).

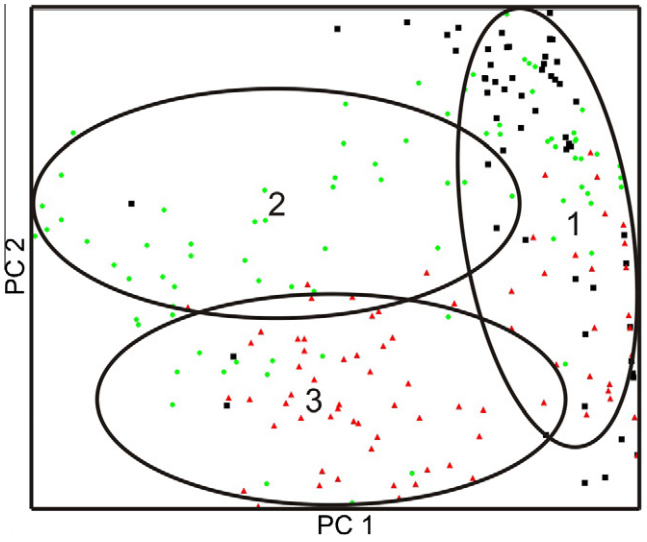

Fig. 7. Differentiated human embryonic stem cells grouped according to their treatments. Principal component analysis clustered the differentiated cells into three groups. AAFBS treated cells (black squares) clustered mainly into group 1, AAB27 treated cells (red dots) into group 2 and AANaB treated cells (green triangles) into group 3. Cells in group 1 were characterized by high expression levels of pluripotency genes (*POU5F1* and *NANOG*) and low expression levels of differentiation genes (*CER1*, *CXCR4*, *FOXA2*, *HHEX*, *LHX1*, *MIXL1* and *SOX17*) (Table 1, Fig. 6 and Fig S5). Cells in group 2 showed high expressions of both pluripotency and differentiation genes, while group 3 cells were characterized by low expression levels of pluripotency genes and intermediate expression levels of differentiation genes. Loadings for principal component analysis are shown in Fig S5. *HNF1B* was excluded from the analysis due to few data points.

4. Discussion

In the attempts of developing protocols for programming pluripotent stem cells towards therapeutically relevant cell types, such as beta-cells and hepatocytes, recapitulating the molecular events along the developmental program of pancreatic and hepatic development are believed to be the most successful strategy. Beta-cells and hepatocytes share a common origin from a bipotent progenitor population of anterior DE cells that have the potential to become both liver and pancreas [48]. In vitro differentiation is by no means a synchronized process. Instead, cell cultures contain a mixture of cells with different degrees of maturation. Detailed single-cell characterization is an important and informative tool to define the expression signature of individual cells in differentiating hESCs cultures, and to compare them to their in vivo counterparts. Here, we differentiated hESCs towards DE with three different methods of activin A treatment. Cell differentiation was evaluated both at cell population and single-cell level, using key marker genes that identify DE with anterior identity.

Most DE markers are not exclusively expressed in DE, but are also expressed in other cell types. Therefore no single marker can be used, instead a panel of markers that collectively identify definitive endoderm and exclude extraembryonic endoderm need to be used. All activin A treatments induced gene expression of anterior DE markers, while the gut endodermal markers AFP and CDX2 were absent, indicating differentiation towards a DE phenotype that has not yet fully developed into gut endoderm. The temporal gene expression profile during AAB27 and especially AANaB differentiation showed similar characteristics as to DE formation in vertebrates (Fig. 2) [14]. Transient expression of *T* and *MIXL1*, which are characteristic markers of PS formation [19,49], were detected before induction of endodermal genes *SOX17, FOXA2* and *CXCR4* (Fig. 2). The gene expression profiles of PS and DE genes indicated that AAB27 and AANaB treatments transitioned cells through a mesendodermal progenitor stage followed by differentiation towards endoderm rather than mesoderm.

Differentiation towards VE or DE was assessed with *CXCR4* and *SOX7* expression. *CXCR4* is expressed in DE but not in VE, while *SOX7* has the opposite expression pattern [23,26]. Upregulation of *CXCR4* gene expression in combination with absence of SOX7 protein expression indicated that AAB27 and AANaB treatments directed hESCs towards DE and not to VE (Figs. 2 and 3 and Figs. S3 and S4).

Cell population analysis implicated that AAB27 and AANaB differentiations, compared to AAFBS treatment, were similar (Fig. 2). The single-cell analysis confirmed this observation. In order to characterize the identity of cells generated during the different activin A treatments, we examined gene expression of anterior DE markers in detail at the single-cell level. Binary analysis showed that AAB27 and AANaB treatments generated similar numbers of cells co-expressing the DE markers: *CER1*, *CXCR4*, *FOXA2*, *HHEX* and *SOX17*. Notably, the *SOX17*$^{+}$ population of AAB27 treated cells co-expressed *MIXL1* and *LHX1* to a higher extent than AANaB treated cells (Tables 1 and 2). In addition, significant correlations between *MIXL1* and *LHX1*, and *LHX1* and *SOX17* were observed in

AAB27 treated cells, but not in AANaB treated cells (Table 3). Furthermore, cells treated with AAB27 expressed *MIXL1* and *LHX1* at higher levels compared to AANaB treated cells (Fig. 6). This observed difference in the *SOX17*$^+$ cell population could not be detected at cell population level (Fig. 1). In vertebrates, *Mixl1* and *Lhx1* are expressed during gastrulation and early somite stages and are involved in commitment towards the endodermal lineage and in anterior movement of the endoderm [20,50]. In this context, the quantified differences in *MIXL1* and *LHX1* expressions and correlations among the *SOX17*$^+$cells led us to speculate that AANaB treated cells have progressed further in differentiation towards gut endoderm than AAB27 treated cells. This hypothesis is further supported by the PCA classification. The PCA showed that most AANaB treated cells grouped separately compared to both AAB27 and AAFBS treated cells. Several DE markers were correlated in AAB27 treated cells at single-cell level, while few correlations were found in AANaB treated cells (Table 3). One explanation for this observation is that AAB27 treated cells were in early stages of DE differentiation and therefore more synchronized than AANaB treated cells. This hypothesis is further supported by relative high expression of pluripotency markers (*POU5F1* and *NANOG*) and PS markers (*T* and *MIXL1*) in AAB27 treated cells compared to AANaB treated cells. POU5F1 and NANOG also bind most DE gene promoters as repressors or suppressors [51]. If some AANaB treated cells have differentiated to more mature cell states, these cultures would most likely contain more cell types than the other treatments, which may explain the few observed transcript correlations at single-cell level for AANaB treated cells (Table 3). The AANaB treated cells were characterized with intermediate expression of anterior DE markers and low expression of pluripotency markers (Table 1, Figs. 6 and 7 and Fig. S5).

Interestingly, no or very weak expression of POU5F1 could be detected by immunostainings for AAB27 and AANaB treated cells, while transcripts for both genes could easily be detected at both cell population and single-cell level (Figs. 2, 4 and 6). This discrepancy may be explained by different levels of sensitivity between immunostainings and reverse transcription quantitative real-time PCR. However, the downregulations of *POU5F1* and *NANOG* transcripts were modest, indicating that post-transcriptional regulation of POU5F1 and NANOG can be the major regulatory mechanism of these pluripotency markers during activin A differentiation. To fully test the lineage potential of DE cells displaying different signatures of anterior DE expression, additional in vitro and in vivo assays are needed [52]. Assays that make it possible to follow cell fate decisions would provide an opportunity to test if cells displaying different molecular signature at the DE stage have the same potential to develop along the endodermal lineage. Such assay could be based on genetic lineage tracing that irreversibly mark cells at one developmental stage and thereafter can be identified in descendants of this early cell type [53,54].

In summary, we applied gene expression profiling at both cell population and single-cell level to monitor in vitro differentiation of hESCs towards DE using three different activin A based treatments. In addition, immunocytochemistry was used to confirm DE differentiation at protein level. To study DE differentiation, a panel of markers was used, since no uniquely expressed DE marker exists. Single-cell analysis allowed us to study differentiation heterogeneity and characterize individual cells, while cell population studies were useful to monitor the overall differentiation pattern. Single-cell analysis revealed distinct gene expression pattern for the three different differentiation protocols applied. Our data illustrate the necessity of using single-cell analysis as a tool to define the characteristics of individual cells. Here, we applied unsupervised algorithms to find unknown subpopulations of cells. This approach allowed us to identify cell states not by the presence of specific markers but rather by expression levels of shared markers. Confirmation of newly found subpopulations with other algorithms is important, since most algorithms will separate cells into groups regardless their importance. We used well-known differentiation markers, which allowed us to interpret data from a developmental point of view. Analysis of genes with unknown functions may generate unexpected correlations and interesting subpopulations for further investigations, but direct interpretations are usually hard and very speculative. Improved analytical tools to characterize different stages of development during in vitro differentiation of pluripotent stem cells will open new avenues to develop and improve current differentiation protocols.

Disclosure

A.S. declares stock ownership in TATAA Biocenter AB. K.N. and A.S. are employed by Cellartis AB.

Acknowledgments

We thank Dr. Nico Heins for valuable scientific communications. We also thank Karin Noaksson, Jens Björkman, Jörg Benecke and Anders Aspegren for excellent technical assistance. This work was partly supported by Grants from Assar Gabrielssons Research Foundation, Johan Jansson Foundation for Cancer Research, Socialstyrelsen, Swedish Society for Medical Research, The Swedish Research Council (A.S., K2012-99X-21954-01-3), The BioCARE National Strategic Research Program at University of Gothenburg, and Wilhelm and Martina Lundgren Foundation for Scientific Research.

Appendix A. Supplementary data

Supplementary data associated with this article can be found, in the online version, at http://dx.doi.org/10.1016/j.ymeth.2012.03.030.

References

[1] J. Ameri, A. Ståhlberg, J. Pedersen, J.K. Johansson, M.M. Johannesson, I. Artner, H. Semb, Stem Cells 28 (2009) 45–56.
[2] M. Borowiak, R. Maehr, S. Chen, A.E. Chen, W. Tang, J.L. Fox, S.L. Schreiber, D. Melton, Cell Stem Cell 4 (2009) 348–358.
[3] K.A. D'Amour, A.D. Agulnick, S. Eliazer, O.G. Kelly, E. Kroon, E.E. Baetge, Nat. Biotechnol. 23 (2005) 1534–1541.
[4] K.A. D'Amour, A.G. Bang, S. Eliazer, O.G. Kelly, A.D. Agulnick, N.G. Smart, M.A. Moorman, E. Kroon, M.K. Carpenter, E.E. Baetge, Nat. Biotechnol. 24 (2006) 1392–1401.
[5] M. Hansson, D.R. Olesen, J.M.L. Peterslund, N. Engberg, M. Kahn, M. Winzi, T. Klein, P. Maddox-Hyttel, P. Serup, Dev. Biol. 330 (2009) 286–304.
[6] J. Jiang, M. Au, K. Lu, A. Eshpeter, G. Korbutt, G. Fisk, A.S. Majumdar, Stem cells 25 (2007) 1940–1953.
[7] M. Johannesson, A. Stahlberg, J. Ameri, F.W. Sand, K. Norrman, H. Semb, PLoS ONE 4 (2009) e4794.
[8] E. Kroon, L.A. Martinson, K. Kadoya, A.G. Bang, O.G. Kelly, S. Eliazer, H. Young, M. Richardson, N.G. Smart, J. Cunningham, et al., Nat. Biotechnol. 26 (2008) 443–452.
[9] G.M. Morrison, I. Oikonomopoulou, R.P. Migueles, S. Soneji, A. Livigni, T. Enver, J.M. Brickman, Cell Stem Cell 3 (2008) 402–415.
[10] B.W. Phillips, H. Hentze, W.L. Rust, Q.P. Chen, H. Chipperfield, E.K. Tan, S. Abraham, A. Sadasivam, P.L. Soong, S.T. Wang, et al., Stem Cells Dev. 16 (2007) 561–578.
[11] D. Zhang, W. Jiang, M. Liu, X. Sui, X. Yin, S. Chen, Y. Shi, H. Deng, Cell Res. 19 (2009) 429–438.
[12] D.C. Hay, D. Zhao, J. Fletcher, Z.A. Hewitt, D. McLean, A. Urruticoechea-Uriguen, J.R. Black, C. Elcombe, J.A. Ross, R. Wolf, et al., Stem cells 26 (2008) 894–902.
[13] P.P.L. Tam, R.R. Behringer, Mech. Dev. 68 (1997) 3–25.
[14] A.M. Zorn, J.M. Wells, Annu. Rev. Cell Dev. Biol. 25 (2009) 221–251.
[15] L.A. Lowe, S. Yamada, M.R. Kuehn, Development 128 (2001) 1831–1843.
[16] S.D. Vincent, N.R. Dunn, S. Hayashi, D.P. Norris, E.J. Robertson, Genes Dev. 17 (2003) 1646–1662.
[17] J.R. Barrow, W.D. Howell, M. Rule, S. Hayashi, K.R. Thomas, M.R. Capecchi, A.P. McMahon, Dev. Biol. 312 (2007) 312–320.
[18] J.A. Rivera-Pérez, T. Magnuson, Dev. Biol. 288 (2005) 363–371.

[19] A.H. Hart, L. Hartley, K. Sourris, E.S. Stadler, R. Li, E.G. Stanley, P.P.L. Tam, A.G. Elefanty, L. Robb, Development 129 (2002) 3597–3608.
[20] P.P.L. Tam, P.L. Khoo, S.L. Lewis, H. Bildsoe, N. Wong, T.E. Tsang, J.M. Gad, L. Robb, Development 134 (2007) 251–260.
[21] S.L. Ang, A. Wierda, D. Wong, K.A. Stevens, S. Cascio, J. Rossant, K.S. Zaret, Development 119 (1993) 1301–1315.
[22] J.A. Belo, T. Bouwmeester, L. Leyns, N. Kertesz, M. Gallo, M. Follettie, E.M. De Robertis, Mech. Dev. 68 (1997) 45–57.
[23] M. Kanai-Azuma, Y. Kanai, J.M. Gad, Y. Tajima, C. Taya, M. Kurohmaru, Y. Sanai, H. Yonekawa, K. Yazaki, P.P.L. Tam, et al., Development 129 (2002) 2367–2379.
[24] K. Dickinson, J. Leonard, J.C. Baker, Dev. Dyn. 235 (2006) 368–381.
[25] A. Fukui, T. Goto, J. Kitamoto, M. Homma, M. Asashima, Biochem. Biophys. Res. Commun. 354 (2007) 472–477.
[26] K.E. McGrath, A.D. Koniski, K.M. Maltby, J.K. McGann, J. Palis, Dev. Biol. 213 (1999) 442–456.
[27] P.Q. Thomas, A. Brown, R.S. Beddington, Development 125 (1998) 85–94.
[28] J.M. Brickman, C.M. Jones, M. Clements, J.C. Smith, R.S. Beddington, Development 127 (2000) 2303–2315.
[29] J.P. Martinez Barbera, M. Clements, P. Thomas, T. Rodriguez, D. Meloy, D. Kioussis, R.S. Beddington, Development 127 (2000) 2433–2445.
[30] W. Shawlot, J.M. Deng, R.R. Behringer, Proc. Natl. Acad. Sci. USA 95 (1998) 6198–6203.
[31] W. Shawlot, M. Wakamiya, K.M. Kwan, A. Kania, T.M. Jessell, R.R. Behringer, Development 126 (1999) 4925–4932.
[32] A. Perea-Gomez, W. Shawlot, H. Sasaki, R.R. Behringer, S. Ang, Development 126 (1999) 4499–4511.
[33] G.S. Kwon, S.T. Fraser, G.S. Eakin, M. Mangano, J. Isern, K.E. Sahr, A.K. Hadjantonakis, M.H. Baron, Dev. Dyn. 235 (2006) 2549–2558.
[34] F. Beck, T. Erler, A. Russell, R. James, Dev. Dyn. 204 (1995) 219–227.
[35] E. Barbacci, M. Reber, M.O. Ott, C. Breillat, F. Huetz, S. Cereghini, Development 126 (1999) 4795–4805.
[36] A. Raj, A. van Oudenaarden, Cell 135 (2008) 216–226.
[37] K.H. Narsinh, N. Sun, V. Sanchez-Freire, A.S. Lee, P. Almeida, S. Hu, T. Jan, K.D. Wilson, D. Leong, J. Rosenberg, et al., J. Clin. Invest. 121 (2011) 1217–1221.
[38] A. Ståhlberg, D. Andersson, J. Aurelius, M. Faiz, M. Pekna, M. Kubista, M. Pekny, Nucleic Acids Res. 39 (2011) e24.
[39] M. Bengtsson, A. Ståhlberg, P. Rorsman, M. Kubista, Genome Res. 15 (2005) 1388–1392.
[40] N. Heins, M.C.O. Englund, C. Sjöblom, U. Dahl, A. Tonning, C. Bergh, A. Lindahl, C. Hanson, H. Semb, Stem Cells 22 (2004) 367–376.
[41] S.A. Bustin, V. Benes, J.A. Garson, J. Hellemans, J. Huggett, M. Kubista, R. Mueller, T. Nolan, M.W. Pfaffl, G.L. Shipley, J. Vandesompele, C.T. Wittwer, Clin. Chem. 55 (2009) 611–622.
[42] A. Ståhlberg, K. Elbing, J. Andrade-Garda, B. Sjögreen, A. Forootan, M. Kubista, BMC Genomics 9 (2008) 170.
[43] A. Ståhlberg, M. Bengtsson, Methods 50 (2010) 282–288.
[44] A. Ståhlberg, M. Bengtsson, M. Hemberg, H. Semb, Clin. Chem. 55 (2009) 2162–2170.
[45] A. Raj, C.S. Peskin, D. Tranchina, D.Y. Vargas, S. Tyagi, PLoS Biol. 4 (2006) e309.
[46] A.C. McPherron, S.J. Lee, The transforming growth factor-beta superfamily, in: D. Leroith, C. Bondy (Eds.), Growth Factors and Cytokines in Health and Disease, JAI Press Inc., Greenwich, 1996, pp. 357–393.
[47] P.P.L. Tam, M. Kanai-Azuma, Y. Kanai, Curr. Opin. Genet. Dev. 13 (2003) 393–400.
[48] G. Deutsch, J. Jung, M. Zheng, J. Lora, K.S. Zaret, Development 128 (2001) 871–881.
[49] R.S.P. Beddington, P. Rashbass, V. Wilson, Development 116 (1992) 157–165.
[50] P.P.L. Tam, P.L. Khoo, N. Wong, T.E. Tsang, R.R. Behringer, Dev. Biol. 274 (2004) 171–187.
[51] L.A. Boyer, T.I. Lee, M.F. Cole, S.E. Johnstone, S.S. Levine, J.P. Zucker, M.G. Guenther, R.M. Kumar, H.L. Murray, R.G. Jenner, et al., Cell 122 (2005) 947–956.
[52] H. Semb, Cell Stem Cell 3 (2008) 355–356.
[53] P.L. Herrera, Int. J. Dev. Biol. 46 (2002) 97–103.
[54] V.M. Scwitzgebel, D.W. Scheel, J.R. Conners, J. Kalamaras, J.E. Lee, D.J. Anderson, L. Sussel, J.D. Johnson, M.S. German, Development 127 (2000) 3533–3542.